Virology 589 (2024) 109921

Contents lists available at ScienceDirect

Virology

journal homepage: www.elsevier.com/locate/virology

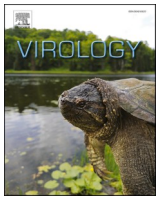

Murine norovirus infection of macrophages induces intrinsic apoptosis as the major form of programmed cell death

Joshua M. Deerain [a,1], Turgut E. Aktepe [a,2], Alice M. Trenerry [a], Gregor Ebert [b,c,3], Jennifer L. Hyde [d], Katelyn Charry [a], Laura Edgington-Mitchell [e], Banyan Xu [e], Rebecca L. Ambrose [f], Soroush T. Sarvestani [a], Kate E. Lawlor [b,c,f,g], Jaclyn S. Pearson [f,g,h], Peter A. White [i], Jason M. Mackenzie [a,*]

[a] Department of Microbiology and Immunology, University of Melbourne, at the Peter Doherty Institute for Infection and Immunity, VIC, 3000, Australia
[b] The Walter and Elisa Hall Institute, Melbourne, VIC, 3052, Australia
[c] Department of Medical Biology, University of Melbourne, VIC, 3050, Australia
[d] Department of Microbiology, School of Medicine, University of Washington, Seattle, USA
[e] Department of Biochemistry and Pharmacology, Bio21 Molecular Science and Biotechnology Institute, The University of Melbourne, Melbourne, VIC, 3010, Australia
[f] Centre for Innate Immunity and Infectious Diseases, Hudson Institute of Medical Research, Melbourne, VIC, 3168, Australia
[g] Department of Molecular and Translational Science, Monash University, Melbourne, VIC, 3168, Australia
[h] Department of Microbiology, Monash University, Melbourne, VIC, 3168, Australia
[i] School of Biotechnology and Biomolecular Sciences, University of New South Wales, Sydney, NSW, 2052, Australia

ARTICLE INFO

Handling Editor: Dr. Jasmine Tomar

Keywords:
Norovirus
Murine norovirus
Apoptosis
Programmed cell death
Macrophage

ABSTRACT

Human norovirus is the leading cause of acute gastroenteritis worldwide, however despite the significance of this pathogen, we have a limited understanding of how noroviruses cause disease, and modulate the innate immune response. Programmed cell death (PCD) is an important part of the innate response to invading pathogens, but little is known about how specific PCD pathways contribute to norovirus replication. Here, we reveal that murine norovirus (MNV) virus-induced PCD in macrophages correlates with the release of infectious virus. We subsequently show, genetically and chemically, that MNV-induced cell death and viral replication occurs independent of the activity of inflammatory mediators. Further analysis revealed that MNV infection promotes the cleavage of apoptotic caspase-3 and PARP. Correspondingly, pan-caspase inhibition, or BAX and BAK deficiency, perturbed viral replication rates and delayed virus release and cell death. These results provide new insights into how MNV harnesses cell death to increase viral burden.

1. Introduction

Noroviruses (NoVs) are non-enveloped, positive sense single-stranded RNA (+ssRNA) viruses belonging to the family *Caliciviridae* (Vinje et al., 2019). Estimates suggest that NoVs are responsible for ~685 million cases in the human population annually, equating to approximately 16–18% of all acute diarrhoeal disease incidences reported worldwide (Ahmed et al., 2014; Liao et al., 2021; Shah and Hall, 2018). While the vast majority of infections are self-limiting and resolved within 48 h, approximately 212,000 deaths are associated with NoV each year making this virus the leading cause of gastroenteritis and gastroenteritis-associated deaths globally (Pires et al., 2015). Despite the significant global health burden, effective antiviral treatments and preventative vaccines remain unavailable. Progress in developing effective therapies has been hampered by the fact that infective human NoVs are difficult to cultivate under laboratory conditions, therefore the closely related murine norovirus (MNV) acts as a suitable model to study human NoV infection *in vivo* and *in vitro* (Wobus et al., 2004).

Investigations with MNV have shown how noroviruses utilise a variety of mechanisms to modulate immune responses to promote

* Corresponding author.
E-mail address: jason.mackenzie@unimelb.edu.au (J.M. Mackenzie).
[1] Present address: Australian Centre for Disease Preparedness (ACDP), East Geelong, VIC, 3219, Australia.
[2] Present address: Melbourne Veterinary School, Faculty of Veterinary and Agricultural Sciences, The University of Melbourne, VIC, 3010, Australia.
[3] Present address: Institute of Virology, Technical University of Munich/Helmholtz Zentrum München, Munich, Germany.

https://doi.org/10.1016/j.virol.2023.109921
Received 5 September 2023; Received in revised form 9 October 2023; Accepted 23 October 2023
Available online 31 October 2023

infection (Fritzlar et al., 2018, 2019; McFadden et al., 2011). Programmed cell death (PCD) is an important part of the innate immune response to infection, allowing cells to undergo regulated cellular suicide in response to a variety of signals. To date several PCD pathways have been implicated in the innate immune response to pathogen infection, with the most characterised being apoptosis, necroptosis and pyroptosis. Pyroptosis occurs as a consequence of inflammasome activation in response to infection or other damage-associated molecular patterns (DAMPs). Specifically, inflammasome activation triggers caspase-1-mediated activation of gasdermin D (GSDMD), releasing the pore-forming p30 fragment that induces transmembrane pore formation and cell lysis. Additionally, caspase-1 promotes cleavage and activation of the proinflammatory cytokines interleukin-1beta (IL-1β) and interleukin 18 (IL-18), driving further inflammation (Bedoui et al., 2020). In the case of Gram-negative bacterial infections, LPS binds and activates caspase-11 to cleave GSDMD leading to pyroptosis and noncanonical activation of the NLRP3 inflammasome (Lee et al., 2018). Necroptosis, is another form of lytic inflammatory cell death that can be triggered upon pathogen or DAMP sensing by immune receptors, including Toll-like receptors, TNF receptor I and the DNA sensing Z-DNA binding protein-1 (ZBP-1) (Seo et al., 2021). Activation of necroptotic signalling leads to phosphorylation and activation of receptor-interacting serine-threonine protein kinase 1 (RIPK1) and RIPK3. RIPK3 then phosphorylates and activates its substrate, the essential necroptotic effector pseudokinase mixed lineage kinase domain like (MLKL). MLKL oligomerises and traffics to the cellular membrane to form lytic pores (Bedoui et al., 2020).

In contrast to pyroptosis and necroptosis, apoptotic cell death is non-immunogenic as it involves the regulated caspase-mediated disintegration of a cell into small fragments, termed apoptotic bodies, that can be silently removed by professional phagocytes. Apoptosis is comprised of two distinct but converging signalling pathways induced by extrinsic and intrinsic stimuli. During extrinsic apoptosis, death receptor ligation on the cell surface results in the proteolytic activation of caspase-8 and subsequent activation of executioner caspases −3 and −7 that induce cellular dismantling. During intrinsic apoptosis, a tightly controlled homeostasis between the pro-survival BCL-2 proteins and pro-apoptotic effectors (BAX and BAK) is disrupted by pro-apoptotic initiators (BH3-only proteins) which sequester the pro-survival proteins and trigger BAX/BAK activation. Additionally, some BH3-only proteins can interact directly with BAX/BAK to induce apoptosis. BAX/BAK activation and oligomerization induces mitochondrial outer membrane permeabilization and the release of cytochrome *c*. This promotes the formation of the apoptosome complex that ultimately results in caspase-9 activation which converges with the extrinsic pathway to activate caspases −3 and −7.

Previous studies into PCD and MNV infection have observed signs of intrinsic apoptosis induction and revealed possible mechanisms for viral modulation including, downregulation of inhibitor of apoptosis family member survivin, upregulation of cathepsin B and virulence factor 1 (VF1) activity (McFadden et al., 2011; Bok et al., 2009; Furman et al., 2009; Herod et al., 2014). It has also been shown that proteolytic processing of MNV NS1/2 relies on apoptosis induction and caspase-3 activity, with key roles in driving intestinal infection, establishing persistence, and evading anti-viral interferon responses (Lee et al., 2019; Robinson et al., 2019). However, it is not clear what other direct impact apoptosis has on replication and the release of MNV. Furthermore, limited work has investigated the contribution of other cell death pathways during norovirus infection, although some recent evidence has emerged to indicate a potential pore-forming role for the NS3 protein (Wang et al., 2023). Noting that an increasing level of cell death plasticity and crosstalk has been described for a range of pathogens (Bedoui et al., 2020; Doerflinger et al., 2020; Sarhan et al., 2018; Orning et al., 2018; Samir et al., 2020).

Herein, we show a comprehensive assessment of four key PCD pathways, namely pyroptosis, necroptosis and extrinsic and intrinsic apoptosis during MNV infection of macrophages *in vitro*. We confirm previous findings that intrinsic apoptosis is induced and describe the requirement for cell death to allow efficient virus replication and release.

2. Materials and methods

2.1. Cells lines

Wild-type, *gsdmd*$^{-/-}$, *gsdmd*$^{-/-}$*bax*$^{-/-}$*bak*$^{-/-}$, and *caspase-1*$^{-/-}$*caspase-11*$^{-/-}$*caspase-12*$^{-/-}$*caspase-8*$^{-/-}$*ripk3*$^{-/-}$ (referred to as *C1*$^{-/-}$*C11*$^{-/-}$*C12*$^{-/-}$*C8*$^{-/-}$*R3*$^{-/-}$) murine immortalised bone marrow-derived macrophages (iBMDM) were kindly provided by Macro Herold at Walter and Elisa Hall Institute, Melbourne, Australia. The phenotypes of these mice have all been previously validated in microbial infection models (Doerflinger et al., 2020). RAW264.7 cells (murine macrophage cell line) were purchased from the ATCC (Manassas, VA, USA). All cell lines were maintained in Dulbecco's Modified Eagle's Medium (DMEM) (Gibco) supplemented with 10% foetal calf serum (FCS) (Gibco), 1% GlutaMAX (200 mM) (Gibco) and 50 U/mL penicillin and 50 μg/mL streptomycin and cultivated at 37 °C in a 5% CO_2 incubator. Primary bone marrow-derived macrophages (pBMDM) were generated by culturing bone marrow cells isolated from the femoral and tibial bones of wild-type C57BL/6 or *caspase-8*$^{-/-}$*ripk1*$^{-/-}$*ripk3*$^{-/-}$, *caspase-8*$^{-/-}$*ripk3*$^{-/-}$, *ripk1*^{D138N}, *ripk3*$^{-/-}$, and *mlkl*$^{-/-}$ mice (on a C57BL/6 background) in bacterial Petri dishes for 6 days in Dulbecco's modified Eagle's medium (DMEM) containing 8% foetal bovine serum, 50 U/mL penicillin and 50 μg/mL streptomycin (complete media) supplemented with 20% L929 conditioned media (37 °C, 5% CO_2) (Lawlor et al., 2015).

2.2. MNV infections and plaque assays

BMDM cells cultured to 80% confluency in 24-well plates were infected with a tertiary stock of MNV CW1 strain at MOI 5 (Karst et al., 2003). Briefly, culture media was removed from cells and MNV in 200 μL serum-free DMEM added and allowed to absorb for 1 h at 37 °C. 300 μL of infection media (DMEM supplemented with 2FCS, 1% GlutaMAX 200 mM) was then added to each well and infected cells returned to incubate at 37 °C, 5% CO_2. At 3 or 6 h intervals, between 6 and 24 h post infection (h.p.i.), cell supernatant was collected, clarified by low-speed centrifugation, an aliquot taken for cell viability assay, and the remainder stored at −80 °C. Cell lysates were also collected as described below. For plaque assays, 1:10 serial dilutions of cell supernatants were prepared in DMEM and 6 dilutions (10^{-2} – 10^{-7}) were used as inoculum in duplicate. RAW264.7 cells, seeded for 70% confluency on the previous day in 12-well plates, were infected with the diluted supernatants for 1 h. Warmed LMP agar overlay (70% DMEM, 2.5% [vol/vol] FCS, 13.3 mM NaHCO3, 22.4 mM HEPES, 200 mM GlutaMAX, and 0.35% [wt/vol] low-melting-point agarose) was added to infected RAW264.7 cells, allowed to solidify at 4 °C for 30 min and cultured for 48 h in at 37 °C in a 5% CO_2 incubator. Subsequently, cells were fixed with 10% formalin for 1 h and plaques visualised by staining remaining cells with toluidine blue.

2.3. Chemical treatments

For chemical inhibition of RIPK1 and pro-apoptotic caspases, iBMDMs were seeded in 24-well plates as described above ~24 h prior to infection. Culture media was removed, and cells infected for 1 h at 37 °C. Following inoculation, infection media containing chemicals were added to cells. For inhibition of RIPK1, Necrostatin-1s (Nec1s; Merk) was diluted to a final concentration of 30 μM. For inhibition of pro-apoptotic caspases, Q-VD-OPh (QVD; R&D systems) was diluted to a final concentration of 10 μM. For inhibition of the proteasome, MG132 (Ready Made Solution; Sigma-Aldrich) was diluted to a final

concentration of 0.5 μM in DMSO. As a vehicle control, DMSO (Sigma-Aldrich) was diluted to the same level as either Nec1s, QVD or MG132. Cell lysates and supernatants were collected at various time-points as described above.

2.4. LDH release cell viability assay

Cell viability of MNV-infected BMDM cells was assessed using CytoTox 96® Non-Radioactive Cytotoxicity assay (Promega) according to the manufacturer's instructions. Briefly, 50 μL of cell supernatant was collected from MNV-infected cells every 3 h between 9 and 24 h post infection. Cell supernatant was incubated with 50 μL CytoTox 96® reagent in a flat-bottom 96-well plate for 20 min before the reaction was stopped and absorbance read at 490 nm.

2.5. Propidium iodide cell viability assay

BMDMs were seeded into a Corning® Costar 96-Well Black Clear-Bottom Plates at 50,000 cells per well, 24 h prior to beginning cell death measurements. MNV at MOI 5 was added to the infection wells and the plate was incubated at 37 °C for 1 h. Propidium iodide (PI) was added, and PI uptake monitored in real-time on a Clariostar Plus Microplate Reader. Appropriate controls were present to ensure the effectiveness of the assay: no cells, cells but no PI, vehicle control, and total cell lysis (10% Triton X-100). The fluorescence of DNA-intercalated propidium iodide at 617 nm was measured every 5 min for 24 h. Data were normalised to uninfected cells and presented as percentage cell viability.

2.6. Western blot

Lysates from MNV-infected cells were harvested on ice for 30 min in KALB lysis buffer [150 mM NaCl, 50 mM Tris-HCl, pH 7.5, 1% (v/v) Triton X-100, 1 mM EDTA] supplemented with 1% Protease Inhibitor cocktail III. Samples were centrifuged to isolate soluble fraction which was diluted in Laemmli sample buffer, heated to 90 °C for 10 min and equal volumes loaded in a 4–12% polyacrylamide gels. Proteins were separated by SDS-PAGE, transferred to a polyvinylidene difluoride membrane, and blocked with 5% skim milk powder in TBS-T (Tris buffered saline plus 0.1% Tween). The following primary antibodies were prepared in 5% BSA/TBS-T and incubated with membrane overnight at 4 °C: Mouse anti-RIPK1 (BD Transduction Laboratories, Cat# 610458), Rabbit anti-RIPK3 (Cell Signaling Technology, Cat# 95702), Rabbit anti-PARP (Cell Signaling Technology, Cat# 9542), Rabbit anti-Cleaved Caspase-3 (Asp175) (Cell Signaling Technology, Cat# 9664), Rabbit anti-Actin (Sigma Aldrich, Cat# A2066), Mouse anti-MNV-VP1 (Sigma Aldrich, Cat# MABF2097), Mouse anti-GAPDH (Abcam, Cat# AB8245), Rabbit anti-Calnexin (Abcam, Cat# AB22595), and Rabbit anti-MNV-NS7 (manufactured and produced by Invitrogen). The following day, primary antibodies were removed, membranes washed three times with TBS-T and secondary antibodies added for 2 h at room temperature. Secondary antibodies used were Donkey anti-Rabbit IgG (H + L) and Goat anti-Mouse IgG (H + L) (Invitrogen, Cat# A16035 and G-21040). Visualisation was performed using Amersham ECL Western Blotting Detection Reagent or Western Lightning Ultra (PerkinElmer) on the GE Healthcare Life Sciences AI600 Imager.

2.7. Light and electron microscopy

For light microscopy: BMDM cells were cultured in a 24-well plate and infected with MNV, or left uninfected according to procedure described above. At 12, 18 or 24 h.p.i. the integrity of the cell monolayer was observed under 10X magnification with DMI4000B Automated Inverted Microscope (Leica Microsystems).

For electron microscopy: RAW264.7 macrophages were infected with MNV and at the indicated time post-infection they were fixed with 3% (w/v) glutaraldehyde in 0.1 M cacodylate buffer for 2 h at room temperature. Resin embedding followed, as described (Wobus et al., 2004). Thin sections were cut on a Leica UC7 ultramicrotome using a Diatome diamond knife and collected on formvar and carbon-coated copper mesh grids. The sections were stained and contrasted with 2% aqueous uranyl acetate and Reynold's lead citrate before being viewing on a JOEL 2010 transmission electron microscope. Images were processed for publication in Adobe Photoshop™.

2.8. Cytokine detection

Briefly, BMDMs were pre-treated with either LPS (100 ng/mL), nigericin (5 μM) or DMEM for 3 h followed by MNV infection in selected wells. Supernatants were collected 16 h.p.i. and assessed for cytokine secretion by ELISA. Mouse TNF-α and IL-1β induction was measured using the Mouse TNF-α ELISA kit (Crux Biolab, Cat# EK-0005) and Mouse IL-1β OptEIA™ ELISA Set (Becton Dickinson, Cat# 559603), respectively, and following the manufacturer's protocol. A FLUOstar OPTIMA plate reader (BMG technologies) was used to measure the OD 450 nm absorbance of the samples and standards.

2.9. Flow cytometry analyses

BMDM cells were infected with MNV for the indicated time periods before being detached and stained with a fixable viability dye (eFluor 780; Invitrogen, United States). The cells were then fixed with 4% (v/v) Paraformaldehyde (PFA) in phosphate buffered saline (PBS) and permeabilised with 0.5% (v/v) Triton-X-100 in PBS. The fixed and permeabilised cells were then immunostained with Rabbit anti-Cleaved Caspase-3 antibodies conjugated with donkey anti-rabbit Alexa flour 488 (Invitrogen, Cat# A-21206). Samples were analysed on a LSRFortessa flow cytometer (BD Bioscience) before data analysis using FlowJo software (version 10.4).

2.10. Caspase activity-based probe

Cells were lysed with hypotonic lysis buffer (50 mM HEPES, pH 7.4, 10 mM KCl, 5 mM MgCl2, 2 mM EDTA, 1 % NP-40, 4 mM DTT) on ice for 20 min. Supernatants were cleared by centrifugation at high speed for 5 min, and 80 μg of protein was labelled with 1 μM LE22, a fluorescent caspase activity-based probe, at 37 °C for 20 min (Edgington et al., 2012). The labelling reaction was stopped by adding 5X sample buffer (50% glycerol, 200 mM Tris-Cl [pH 6.8], 10% SDS, 0.05% bromophenol blue, 6.25% 2-ME) followed by heating at 95 °C for 5 min. Proteins were resolved on a 15% SDS-PAGE gel, and the gel was scanned for Cy5 fluorescence using a Typhoon scanner (GE Healthcare). For VP1 immunoblots, proteins were transferred to nitrocellulose membranes and probed with mouse anti-VP1 and rabbit anti-actin (Sigma-Aldrich) Antibodies. After washing with PBS containing 0.05% Tween 20, blots were incubated with donkey anti-mouse 647 (Invitrogen) and goat anti-rabbit IRDye 800CW (LICOR Biosciences). Blots were scanned on a Typhoon scanner (GE Healthcare) using Cy5 and IRlong filters, respectively.

2.11. Immunoprecipitation of caspase-3

Lysates from the 24 h.p.i sample previously labelled with LE22, were solubilized with 5X sample buffer, and boiled as indicated above. The lysates were divided into input and pulldown, each containing ~40 μg in 10 μL volume. 500 μL immunoprecipitation (IP) buffer (PBS, pH7.4, 0.5% NP-40, 1 mM EDTA) was added to the pulldown sample. Protein A/G agarose beads (Santa Cruz Biotechnology; 40 μL slurry) were washed using IP buffer and then added to the pulldown sample along with 5 μL anti-cleaved caspase 3 antibodies (Abcam ab2302) on ice. The mixture was rotated overnight at 4 °C. The beads were washed using IP buffer four times and once with 0.9% NaCl. The remaining NaCl was

removed using an insulin syringe, and 2.5x sample buffer was added. The beads were boiled before running on the gel to elute immunoprecipitated proteins. Proteins were then resolved on an SDS-PAGE gel, as indicated above. The gel was scanned for Cy5 fluorescence using a Typhoon scanner (GE Healthcare).

3. Results

3.1. Bone marrow-derived macrophages undergo a rapid loss of cell viability over the course of MNV infection that is associated with infectious virus release

During our many experiments with MNV we (like others) have consistently observed that MNV infection of macrophages results in loss of cell viability. Morphologically, over the course of MNV infection of macrophages at 18 and 24 h post infection (h.p.i), we observed by electron microscopy hallmark signs of apoptosis, including membrane blebbing and condensation of the nucleus (Fig. 1Ai, ii and iv). In addition, many infected cells displayed necrosis and a clear destruction of cellular architecture (Fig. 1Aiii and iv). These morphological changes were not apparent in mock-infected cells (Fig. 1Av and vi). Due to these ultrastructural observations we next aimed to determine the kinetic impact of macrophage cell death on MNV production over the course of a 24-h infection cycle.

We observed MNV-induced cytopathic effects (CPE) by light microscopy and identified changes in cell viability at 12 h.p.i. that progressed significantly until 24 h.p.i whereupon very few iBMDMs remained adherent to the cell culture plate (Fig. 1B). To extend these observations we utilised a propidium iodide uptake assay which dynamically measures cell viability over extended time frames and in real time. In line with the virus-induced CPE observations (Fig. 1B), macrophage viability rapidly decreased from ~9 h.p.i. and that almost complete loss of cell viability was observed at ~18 h.p.i. (Fig. 1C).

To determine the relationship between cell death and infectious load, we measured the production of infectious virus over a similar time frame by plaque assay. We observed some early MNV production associated with minimal cell death at 6 h.p.i. however, viral production and release peaked at ~18 h.p.i. and then plateaued by 24 h.p.i. (Fig. 1D). These observations indicate that the induction of cell death in infected macrophages was closely associated with the rapid production and accumulation of infectious virus in the cell supernatant. We thus hypothesise that the release of MNV is tightly linked with the loss of cell viability and cell death.

3.2. Cell death observed during MNV infection is not induced by necroptosis

Considering recent reports surrounding the plasticity in PCD pathways engaged by infectious pathogens we next attempted to define the modes engaged during MNV infection. Initially, we investigated the impact of necroptosis on MNV-induced CPE (Fig. 2) by analysing levels the levels of the kinases RIPK1 and RIPK3 that play crucial roles in the induction and activation of the necroptosis pathway (Bedoui et al., 2020). Strikingly, we observed a substantial reduction in the levels of RIPK1 protein between 12 and 18 h.p.i. in the MNV-infected iBMDMs, and almost complete absence by 24 h.p.i. (Fig. 2A and C). Notably, we also observed a similar reduction in the level of the essential necroptotic kinase RIPK3, which can trigger necroptotic cell death in the absence of RIPK1 (Dillon et al., 2014) (Fig. 2B and C). These observations suggest that MNV infection depletes key necroptotic activators RIPK1 and RIPK3 to prevent necroptotic cell death during infection, akin to reports with other pathogens (Harris et al., 2015; Pearson et al., 2017).

To confirm that MNV infection does not trigger necroptosis in infected iBMDMs, we chemically inhibited RIPK1 activity using the compound necrostatin-1s, at a concentration shown to prevent necroptotic cell death (Fig. S1), and assessed virus output via plaque assay. Chemical inhibition of RIPK1 did not impact the growth kinetics of MNV when compared to untreated or vehicle (DMSO) treated cells (Fig. 2D), suggesting that MNV infection does not trigger necroptotic control of virus production. To consolidate this finding, we infected pBMDMs from mice expressing a kinase-inactive mutant RIPK1 (D138 N) (Polykratis et al., 2014) and mice deficient in the essential necroptotic proteins *ripk3* and *mlkl*. Again, we observed minimal impact on virus replication and production in these necroptosis-deficient macrophages (Fig. 2E), supporting our previous observations that necroptosis does not regulate MNV infection.

Overall, these results strongly indicate that MNV does not induce necroptosis to promote dissemination, nor is it engaged by the host to promote pathogen elimination.

3.3. Cell death observed during MNV infection is not induced by pyroptosis

Pyroptosis is a form of inflammatory cell death characterised by permeabilization of the host cell membrane and release of IL-1β (Bedoui et al., 2020). Previously, we observed that MNV induced NLRP3 inflammasome activation and GSDMD-driven pyroptosis in mice and cells that were deficient in *stat-1* (Dubois et al., 2019). However, robust activation of pyroptosis was not observed during MNV infection of unprimed wild-type BMDMs *in vitro*. Therefore, we initially sought to evaluate the release of IL-1β and Tumour necrosis factor-alpha (TNFα) by ELISA from MNV-infected WT or pyroptosis deficient murine iBMDMs with or without stimulation with lipopolysaccharide (LPS) priming to induce inflammasome machinery (Fig. 3A–F). As we previously observed, MNV infection of unprimed WT iBMDM induced minimal secretion of IL-1β and TNFα into the supernatant (Fritzlar et al., 2019). In comparison, LPS priming enhanced cytokine responses and we observed that the release of IL-1β was associated with inflammasome activity, as cells deficient in *caspase-1* or *nlrp3* did not secrete IL-1β in response to either MNV infection or canonical NLRP3 trigger nigericin (Fig. 3A–C). In contrast, TNFα was induced efficiently from all cells under all conditions, with the exception of MNV infection alone (Fig. 3D–F).

To determine if inflammasome-associated pyroptosis contributed to MNV infectious burden, we infected iBMDMs deficient in the pyroptotic effector, *gsdmd*, with MNV and monitored for the production and secretion of infectious virus and cell viability from 9 to 24 h.p.i. (Fig. 3G and H). We observed no discernible change in virus production in *gsdmd*$^{-/-}$ iBMDMs compared to wild-type cells, nor was there any alteration virus-induced cell death kinetics.

Overall, these results support the conclusion that along with necroptosis, pyroptosis does not impact MNV-induced cell death nor the production of infectious virus.

3.4. Apoptosis is induced in response to MNV infection

A limited number of previous studies have shown that apoptosis is induced in response to MNV infection in immortalised macrophages (McFadden et al., 2011; Bok et al., 2009; Furman et al., 2009; Herod et al., 2014). However, the consequence of apoptosis induction on MNV replication has not been extensively assessed. To evaluate this, cellular lysates from MNV-infected iBMDMs (Fig. 4A) were assessed by immunoblot for prototypical markers of apoptosis, namely, cleavage of the DNA repair protein Poly (ADP-ribose) polymerase (PARP) and terminal effector caspase, caspase-3. Over the course of the infection, we observed a significant increase in PARP cleavage that was associated with increased levels of cleaved caspase-3, particularly at 18 h.p.i. (Fig. 4A).

To confirm the activation of apoptotic caspases were engaged upon MNV infection, we evaluated the increase in cleaved caspase-3 by FACS analysis over the course of infection (Fig. 4B). We observed a steady and consistent increase in the abundance of detectable cleaved caspase-3

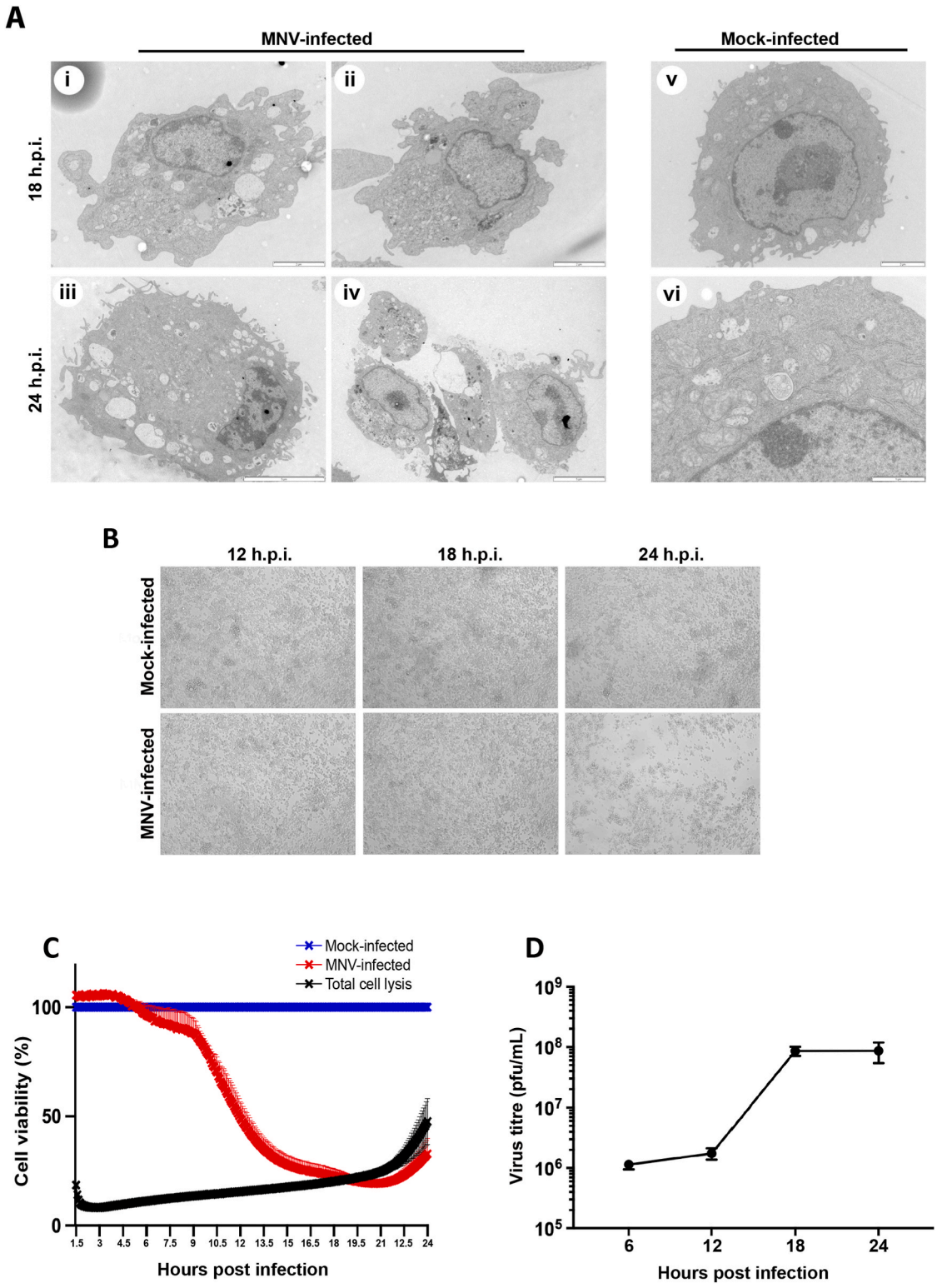

Fig. 1. MNV infection induces rapid loss of cell viability. (A) Transmission electron microscopy images of MNV- or mock-infected (panels v and vi) murine macrophages at 18 (panels i and ii) and 24 h (panels iii and iv) post infection (h.p.i.) highlighting features of apoptosis such as membrane blebbing, nuclear condensation and signs of cellular necrosis. Magnification bars represent 1 μm in panel vi; 2 μm in panels i, ii and v; and 5 μm in panels iii and iv. (B) Brightfield microscopy of iBMDMs either infected with MNV or left uninfected (Mock-infected). Images captured at 5x magnification at 12, 18 or 24 h.p.i. (C) Propidium iodide uptake assay. iBMDMs were uninfected, infected with MNV (MOI of 5) or left uninfected but treated with total cell lysis buffer (10% Triton X-100). Cell viability was assessed by DNA-intercalated propidium iodide fluorescence quantification (5 min intervals) over 24 h.p.i. Cell viability of infected and treated cells was normalised to uninfected cells. Graph depicts the average of 3 replicates from 3 independent experiments and error bars depict ± SEM (D) MNV replication assay. Infectious virus in supernatant from iBMDMs infected with MNV (MOI 5) for 6, 12, 18 or 24 h post infection was quantified by plaque assay. Graph depicts the average of 3 independent experiments and error bars depict ± SEM.

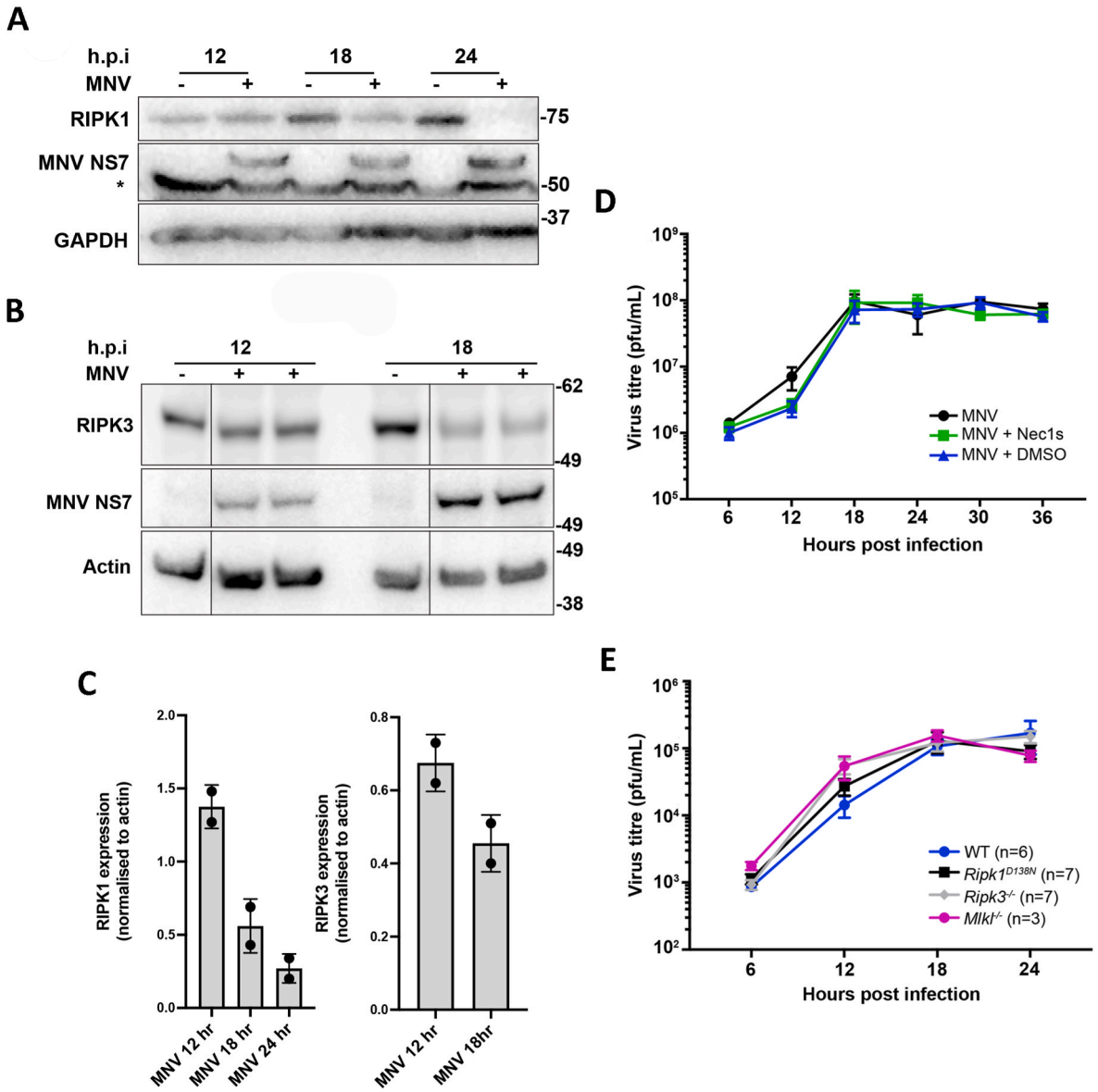

Fig. 2. Inhibition of necroptosis does not impact MNV replication. (A) iBMDMs were either infected with MNV (MOI 5) or left uninfected for 12, 18 or 24 h post infection (h.p.i) before cell lysates were harvested. Immunoblot was performed and membranes immunostained with anti-RIPK1, anti-MNV (NS7) and anti-GAPDH antibodies. (B) Cell lysates from iBMDMs infected with MNV (MOI 5) or left uninfected 12 or 18 h.p.i. were immunoblotted and stained with anti-RIPK3, anti-MNV (NS7) and anti-actin. Lines indicate where the image of a single membrane has been edited to remove irrelevant lanes. (C) Quantitation of the expression levels of RIPK1 and RIPK3 in MNV-infected cells as assessed by Western blot, n = 2, Error bars depict ±SEM. (D) iBMDMs were infected with MNV (MOI of 5) and treated with Necrostatin-1s (Nec1s; 30 μM), DMSO or left untreated. At 6, 12, 18 and 24 h post infection (h.p.i.), supernatants were collected, and virus titre determined by plaque assay. *t*-test was performed with no statistical significance observed between samples at any timepoint. Graph depicts the mean of 2 replicates with error bars showing ±SEM. (E) pBMDMs were harvested from WT, *ripk1*^{D138N}, *ripk3*$^{-/-}$ or *mlkl*$^{-/-}$ C57BL/6 mice. Cells from individual mice were infected with MNV (MOI of 5) and supernatants collected at 6, 12, 18 and 24 h post infection. Virus titre was quantified by plaque assay. For each genetic background viral replication in cells from a minimum of 3 mice were assessed as indicated on graph. A *t*-test was performed with no statistical significance observed between samples at any timepoint. Error bars depict ±SEM.

that correlated with our results by western blotting (Fig. 4A). In addition, we utilised the LE22 activity-based probe, which binds to with active caspase-3, -6 and -7 (Fig. 4C). We observed a significant increase in LE22 labeling from 12 h.p.i. indicating that caspase activation accumulates from this time point. To confirm the specificity of the probe, we immunoprecipitated caspase-3 from LE22-labelled 24 h.p.i. lysates and observed that a vast majority of the signal was associated with caspase-3 (Fig. 4D). These results suggests that MNV infection triggers a significant activation of caspase-3 from 12 h.p.i.

Apoptosis is driven by the extrinsic and intrinsic apoptosis pathways that converge on effector caspase-3, -6 and -7 activation (Bedoui et al., 2020). In the extrinsic pathway, ligation of death receptors or specialised innate immune receptors (e.g. TLR3/4, ZBP1) triggers activation of a death-inducing complex comprising RIPK1, RIPK3, FADD and caspase-8 that precipitates caspase-8 activation and downstream caspase activity. As deletion of the *caspase-8* gene alone induces embryonic lethal necroptotic signalling (Dillon et al., 2014), we examined MNV infection responses in pBMDMs generated from caspase-8 deficient mice on a RIPK1- and/or RIPK3-deficient background, which prevents damaging inflammation (i.e. *casp8*$^{-/-}$*ripk3*$^{-/-}$ or *casp8*$^{-/-}$*ripk3*$^{-/-}$*ripk1*$^{-/-}$). Interestingly, we observed no difference in viral growth kinetics between MNV-infected WT and extrinsic apoptotic

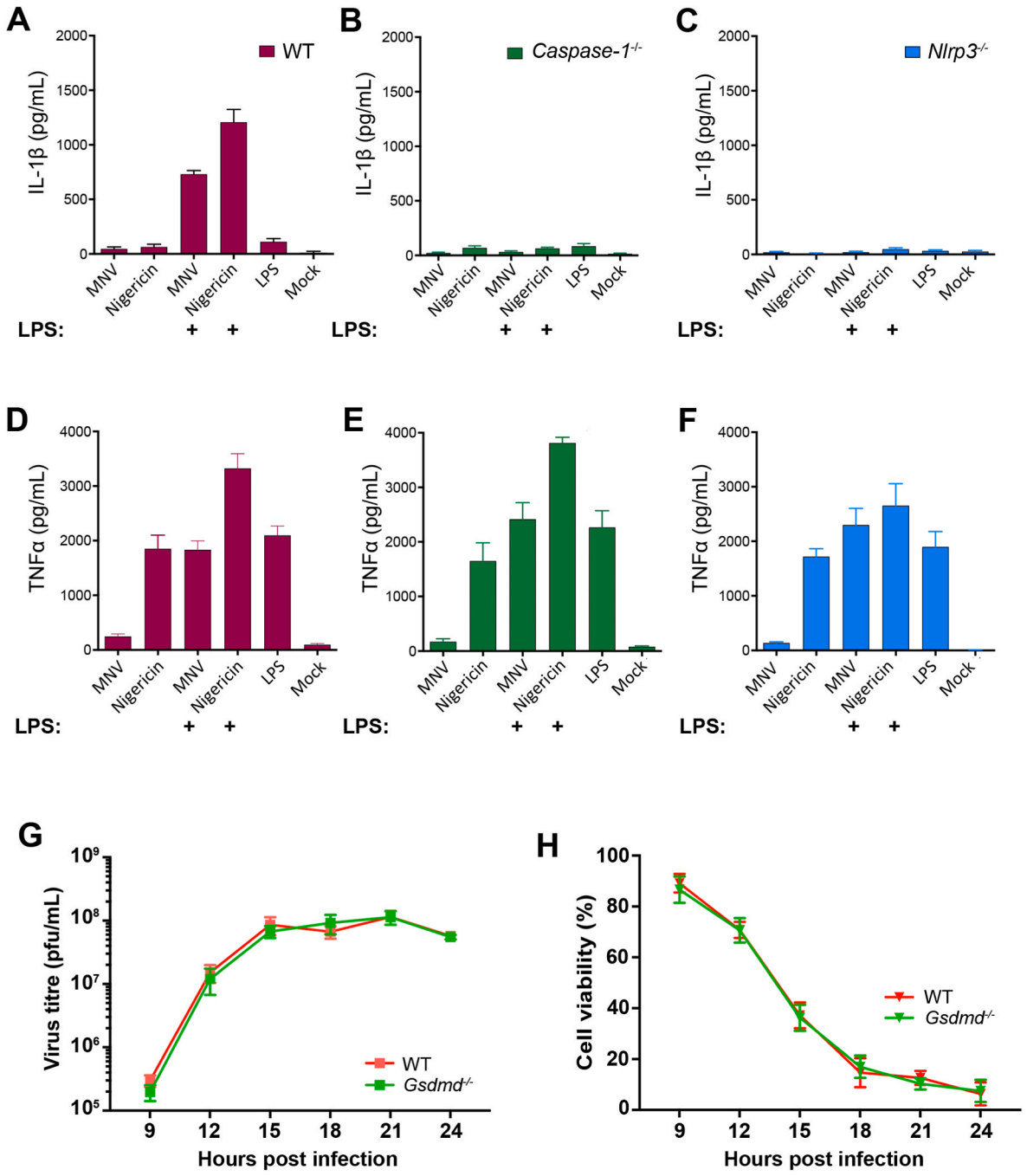

Fig. 3. Inhibition of pyroptosis does not impact MNV replication. WT (A and D), *caspase-1*$^{-/-}$ (B and E) or *nlrp3*$^{-/-}$ (C and F) deficient iBMDMs were infected with MNV (MOI 5) with or without LPS and/or nigericin priming. Supernatants were collected at 16 h.p.i. and subsequently analysed for secreted IL-1β (A, B, C) or TNFα (D, E, F) by ELISA. Error bars depict ±SEM. (G and H) WT or *gsdmd* $^{-/-}$ iBMDM cells were infected with MNV (MOI 5) and supernatants collected at 3-h intervals between 9 and 24 h.p.i. (G) Virus titres were quantified by plaque assay. (H) Cell viability was assessed by LDH release assay. For panels G and H, a *t*-test was performed, and no statistical significance observed between samples at any timepoint. Mean ± SEM of 4 independent experiments is shown.

caspase-8 deficient pBMDMs (Fig. 4E).

Collectively, our observations suggest that MNV infection does not trigger extrinsic apoptotic cell death but is likely to signal cell demise via the intrinsic pathway.

3.5. Inhibition of intrinsic apoptosis limits viral replication and virus-induced cell death

Following our observations that MNV-induced macrophage cell death showed all the morphological and cellular hallmarks of apoptosis (Figs. 1 and 4A–D) but was not extrinsic in nature, we next aimed to qualify the contribution of intrinsic cell death and apoptotic caspases to MNV-mediated cell death responses using the pan-caspase inhibitor Q-VD-OPh. Impressively, pan-caspase inhibition significantly delayed the viral growth in MNV-infected WT iBMDMs (Fig. 5A), reducing the viral burden (~1 log less virus at 15 and 18 h.p.i.) and was associated with a ~ 3 h delay in cell death (Fig. 5B). It is important to note that, despite the caspase inhibition delaying apoptosis, by 24 h.p.i. most cells had lost viability and the level of virus production was similar to untreated cells.

To directly assess the impact of intrinsic apoptosis on MNV replication, we next sought to determine the contribution of the BCL-2 family members and mitochondrial executioners BAX and BAK using iBMDMs

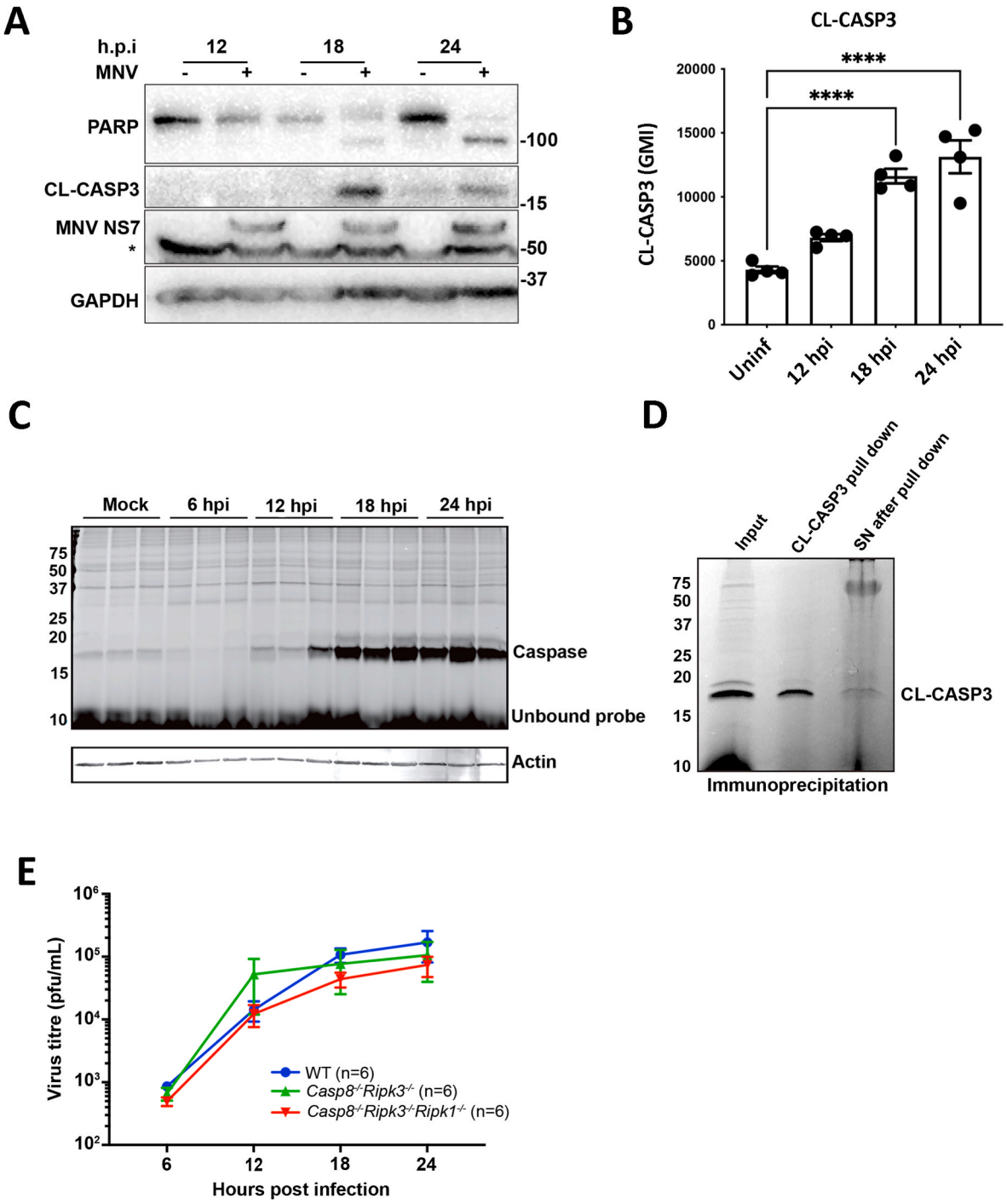

Fig. 4. Apoptosis is induced during infection with MNV. (A) Cell lysates from iBMDMs infected with MNV (MOI 5) or left uninfected for 12, 18 or 24 h post infection were immunoblotted and stained with anti-PARP, anti-CL-CASP3, anti-MNV (NS7), and anti-GAPDH antibodies. Asterisks denotes a non-specific band observed with anti-MNV (NS7) antibody. (B) MNV-infected iBMDMs were fixed at different times post-infection, permeabilised and stained with anti-CL-CASP3 antibodies and species-specific IgG conjugated to AF488 and analysed by flow cytometry. (C) Fluorescent SDS-PAGE of LE22-labelled MNV lysates. iBMDMs were infected with MNV (MOI 5) and cells were harvested at the indicated time points. Lysates were then labelled with the LE22 activity-based probe and proteins were resolved by SDS-PAGE and scanned for Cy5 fluorescence. (D) 24 h.p.i. lysates from panel C were immunoprecipitated with antibodies to caspase-3 and the input, pull-down and residual after pull-down is shown. (E) pBMDMs harvested from individual WT, *casp8*$^{-/-}$*ripk3*$^{-/-}$ or *casp8*$^{-/-}$*ripk3*$^{-/-}$*ripk1*$^{-/-}$ C57BL/6 mice were infected with MNV (MOI 5) and supernatants collected at 6, 12, 18 and 24 h.p.i. Virus titre in supernatants were quantified by plaque assay. For each genetic background viral replication in pBMDMs from 6 mice were assessed. A *t*-test was performed with no statistical significance observed between samples at any timepoint. Error bars depict ±SEM.

deficient for BAX, BAK and GSDMD (*bax*$^{-/-}$*bak*$^{-/-}$*gsdmd*$^{-/-}$). Noting that BAX/BAK doubly deficient macrophages were not readily available, and we had already shown that GSDMD deficiency did not effect MNV infectious outcomes (Fig. 3G and H). Unexpectedly, during the course of infection, we only observed a trend towards a minor delay in the production of infectious virus in *bax*$^{-/-}$*bak*$^{-/-}$*gsdmd*$^{-/-}$ iBMDMs, compared to WT iBMDMs (Fig. 5C). However, we did observe a significant delay in cell death at 12 h.p.i in the absence of BAX and BAK

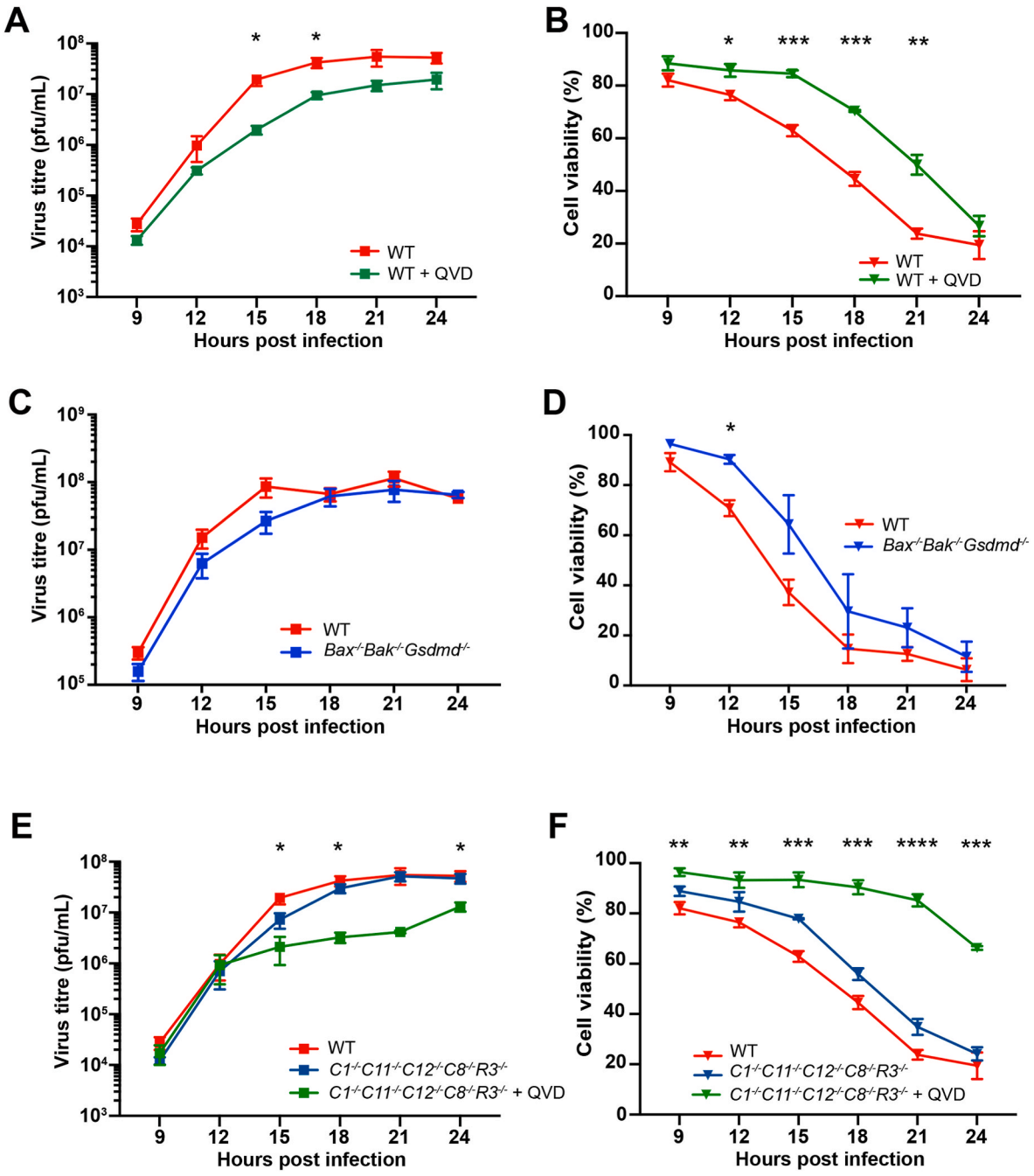

Fig. 5. Inhibition of apoptosis limits MNV replication. (A,B) WT iBMDMs were infected with MNV and either treated with Q-OPH-VD (QVD; 10 μM) or left untreated. At times indicated supernatants were collected and (A) virus titre determined by plaque assay or (B) cell viability determined by LDH release assay. Error bars depict ±SEM from 3 independent experiments. (C–D) WT or *bax*$^{-/-}$*bak*$^{-/-}$*gsdmd*$^{-/-}$ iBMDMs were infected with MNV and supernatants collected at the indicated times. (C) virus titre determined by plaque assay and (D) cell viability determined by LDH release assay. Error bars depict ±SEM from 4 independent experiments. (E–F) WT or *caspase1*$^{-/-}$*caspase11*$^{-/-}$*caspase12*$^{-/-}$*caspase8*$^{-/-}$*ripk3*$^{-/-}$ (*C1*$^{-/-}$*C11*$^{-/-}$*C12*$^{-/-}$*C8*$^{-/-}$*R3*$^{-/-}$) iBMDMs were infected with MNV and either treated with QVD (10 μM) or left untreated. At 3-h intervals post infection supernatants were collected and (E) virus titre determined by plaque assay or (F) cell viability determined by LDH release assay. Error bars depict ±SEM from 3 independent experiments. For each panel *t*-test was used to calculate statistical significance between WT and treatment group for each timepoint (P-value <0.05 *; <0.01 **; <0.001 ***; <0.0001 ****; not significant is unmarked).

activity (Fig. 5D). In line with pan-caspase inhibition with Q-VD-OPh only delaying events, *bax*$^{-/-}$*bak*$^{-/-}$*gsdmd*$^{-/-}$ iBMDMs were killed and produced comparable virus titres at 24 h post infection.

To assess whether BAX and BAK were ultimately functionally redundant during MNV infection and whether other cell death modalities were compensating, we next assessed MNV induced responses in macrophages that were deficient in key proteins required for pyroptosis (*caspase-1, caspase-11*), death receptor-induced apoptosis (*caspase-8*), Endoplasmic reticulum (ER) stress-mediated apoptosis (*caspase-12*) and necroptosis (*ripk3*) (Doerflinger et al., 2020). We again observed no significant difference in viral growth or cell death kinetics in *caspase-1*$^{-/-}$*caspase-11*$^{-/-}$*caspase-12*$^{-/-}$*caspase-8*$^{-/-}$*ripk3*$^{-/-}$ iBMDMs (referred to as *C1*$^{-/-}$*C11*$^{-/-}$*C12*$^{-/-}$*C8*$^{-/-}$*R3*$^{-/-}$), compared with WT iBMDMs (Fig. 5E), which fits with our findings that necroptosis, pyroptosis and extrinsic apoptosis are not required for infected cell demise or MNV replication kinetics. However, pre-treatment of

C1$^{-/-}$*C11*$^{-/-}$*C12*$^{-/-}$*C8*$^{-/-}$*R3*$^{-/-}$ iBMDMs with Q-VD-OPh induced a substantial decrease (greater than 1 log) in virus production at 15 h.p.i. (Fig. 5E), and, even more remarkably, protected macrophages against cell death (Fig. 5F). We hypothesise that this observation indicates crosstalk between alternative cell death pathways mediated via caspase activity. It is worth mentioning that although cell viability was restored to ~70% in Q-VD-OPh treated *C1*$^{-/-}$*C11*$^{-/-}$*C12*$^{-/-}$*C8*$^{-/-}$*R3*$^{-/-}$ iBMDMs, virus recovery was only impacted by ~0.5 log at the very late stage of infection. This suggests that virus release may occur via an alternate mechanism in addition to cell lysis.

4. Discussion

Our understanding of PCD during norovirus infection is extremely limited with only a small number of previous studies attempting to characterise the pathways involved. Herein, we aimed to thoroughly assess the activation of different PCD pathways and describe their effects on viral replication, using MNV as the model for infection. In this study we have shown that PCD is triggered by MNV infection and is involved in virus replication and release. Importantly, we showed that apoptosis, rather than pyroptosis and necroptosis, is the primary PCD pathway activated and is required for the efficient replication of MNV (Fig. 4). Our findings that MNV-induced apoptotic cell death occurs independent of caspases-8 and -12 activity but is partially dependent on the pro-apoptotic proteins BAX and BAK, points to the involvement of the intrinsic apoptotic program, which is consistent with previous reports that caspase-9 cleavage leads to intrinsic apoptosis (Bok et al., 2009).

The long-standing model of non-enveloped virus replication suggests that cell death is required for release of virions. While more recent reports have challenged this paradigm (Santiana et al., 2018), caspase-dependent apoptosis as a mechanism for viral egress has been observed for many non-enveloped enteric viruses including members of *Picornaviridae*, *Reoviridae*, *Caliciviridae* and *Hepeviridae* (Owusu et al., 2021). Induction of apoptosis by MNV has been observed previously (McFadden et al., 2011; Bok et al., 2009; Furman et al., 2009; Herod et al., 2014; Robinson et al., 2019), and while the potential contribution of apoptosis to viral release has been alluded to, no direct assessment has been reported. In our study, we observed that the release of progeny virus was tightly linked to a loss in cellular viability (Fig. 1), strongly suggesting that apoptosis is a key aspect of the viral life cycle. The importance of this for optimal virus replication is further highlighted by multiple reports outlining independent mechanisms for apoptosis modulation, including the downregulation of anti-apoptotic proteins Survivin (Bedoui et al., 2020), activation of pro-apoptotic protease cathepsin B (Furman et al., 2009) and expression of an immunomodulatory protein VF1 (McFadden et al., 2011).

During MNV infection, translation of open reading frame 1 produces a polyprotein consisting of the 7 non-structural viral proteins. Apart from the NS1/2 cleavage site, the large polyprotein is processed into individual proteins by a viral protease. However, a caspase-3 cleavage site is located between NS1/2 requiring the activation of the apoptosis-linked host protease to process (Sosnovtsev et al., 2006). Recent reports have identified this cleavage event and resulting mature NS1 as being key to the virus' ability to establish infection in intestinal epithelial cells, suppress interferon responses, undergo persistent shedding and amplify caspase activity (Lee et al., 2019; Robinson et al., 2019). While the strain of MNV (CW1) used in this study does not require cleavage of NS1/2 for replication, it is important to recognise that the essential and specific induction of apoptosis observed serves a multipurpose approach in promoting MNV infection. Furthermore, in our system we focused on infection of myeloid cells while these previous reports have suggested caspase-dependent processing of NS1/2 processing is required for intestinal epithelial cell tropism.

Recently, it was shown that the viral encoded protein NS3 has the capacity to localise to the mitochondria and potentially permeabilise the mitochondrial membrane via a MLKL-like pore-forming domain (Wang et al., 2023). Although we did not investigate perturbation of the mitochondria in this study, our recent analyses have revealed that NS3 can attenuate host protein translation that results in the depletion of pro-survival proteins thereby driving the infection cell into apoptosis (Aktepe et al., 2023). Both our study and the study by Wang et al., have implicated NS3 in mediating cell death however the potential mechanisms may be slightly different or even occurring at different temporal stages during infection. Further work using *in vivo* infections of apoptosis-deficient mice is required to understand the complex interplay between cell types and confirm our findings.

Inhibition of the alternate PCD pathways, pyroptosis and necroptosis did not alter the kinetics of viral release and cell death during MNV infection (Figs. 2 and 3) suggesting limited contributions of these pathways to promoting/controlling viral replication. Interestingly, key mediators of necroptosis RIPK1 and RIPK3 were found to be depleted in response to infection by MNV (Fig. 2). This is indicative of active prevention of necroptosis by MNV during infection. Other enteric pathogens including the virus Coxsackievirus B3 and bacteria *Escherichia coli* (EPEC) have been shown to limit necroptosis-induced cell death by cleaving RIPK1 and RIPK3 (Harris et al., 2015; Pearson et al., 2017). The mechanism by which this occurred was not extensively explored as part of our study, but no cleavage products were evident. Previous work by our group and others have shown that MNV can limit translation of host proteins to evade the innate immune response (Fritzlar et al., 2019), so one could speculate that this may be a contributing factor to the eventual loss of these key necroptosis proteins.

We saw no evidence that MNV actively triggers pyroptosis in our study. This contrasts with our recent work with collaborators that showed that canonical NLRP3 inflammasome-associated caspase-1 and GSDMD activity mediates early pyroptosis during MNV infection and contributes to the immunopathology observed in a STAT1-deficient mouse model (Dubois et al., 2019). However, consistent with our findings, maturation of IL-1β was not observed upon infection without Toll-Like Receptors 2 or 4-induced inflammasome priming. Crucially, despite these differences in cell death kinetics, both studies report no impact on MNV replication in pyroptosis-deficient BMDMs. Whilst we do not discount caspase-1 mediated pyroptosis contributing to NoV cell death and replication, our findings support the idea that intrinsic apoptosis is the primary cell death pathway activated and required for efficient replication.

It is important to note, that our study has also highlighted significant redundancy, and possible plasticity, in the cell death pathways triggered upon MNV infection, as pan-caspase inhibition or BAX/BAK loss only delayed cell death and virus production. However, treatment of macrophages deficient in extrinsic apoptosis, necroptosis and pyroptosis with a pan-caspase inhibitor most effectively blocked replication and cell death during infection. We also note that caspases-9, 3 and 7 can still be activated in the absence of caspases-1, 11, 12, 8 and Ripk3 so the effect of pan-caspase inhibition could be affecting caspases-9, 3 and 7. We are currently aiming to investigate the roles of these caspases during MNV infection, but also cannot discount any potential non-canonical roles for the caspases. Alternatively we could be observed a modified induction of cell death such as the recently identified PANoptosis that shows hallmarks of pyroptosis, apoptosis and necroptosis, but not necessarily any of these pathways individually (Shi et al., 2023). Further work is obviously required to evaluate this potential phenomenon.

Similar findings have been shown with other intracellular pathogens, notably the bacterial gastrointestinal pathogen, *Salmonella enterica*, where extensive cross-talk between pyroptotic and apoptotic pathways has been observed (Doerflinger et al., 2020). In particular, they observed that activation of caspases-1 and -8 could kill *Salmonella*-infected macrophages in the absence of all other known PCD effectors, highlighting the complexity and redundancy in these pathways. Therefore, while the other PCD pathways assessed did not appear to have a primary role in the replication of MNV, their induction may play a key role to promote viral dissemination. Presumably, this redundancy would not serve the

additional purpose of NS1/2 cleavage and therefore limit the tropism and replication of some MNV strains *in vivo*.

5. Conclusions

Taken together, these findings indicate a preferential activation of apoptosis by MNV during infection. Ongoing work is required to understand the tight regulation of this cell death pathway and to understand if targeted modulation can be used to treat infections. Furthermore, it is still unclear which viral protein and mechanism is employed to regulate cell death during infection with MNV.

CRediT authorship contribution statement

Joshua M. Deerain: Investigation, Validation, Formal analysis, Writing – original draft. **Turgut E. Aktepe:** Investigation, Validation, Formal analysis, Writing – original draft. **Alice M. Trenerry:** Investigation. **Gregor Ebert:** Methodology, Resources, Formal analysis. **Jennifer L. Hyde:** Investigation, Validation, Formal analysis. **Katelyn Charry:** Investigation, Validation. **Laura Edgington-Mitchell:** Validation, Resources, Formal analysis, Writing – review & editing. **Banyan Xu:** Methodology, Validation, Resources. **Rebecca L. Ambrose:** Investigation, Validation, Formal analysis. **Soroush T. Sarvestani:** Investigation, Validation, Formal analysis. **Kate E. Lawlor:** Resources. **Jaclyn S. Pearson:** Investigation, Conceptualization, Methodology, Resources, Supervision, Writing – review & editing, Formal analysis. **Peter A. White:** Conceptualization, Supervision, Writing – review & editing, Funding acquisition. **Jason M. Mackenzie:** Investigation, Conceptualization, Methodology, Resources, Supervision, Writing – original draft, Formal analysis, Funding acquisition.

Declaration of competing interest

The authors declare that they have no known competing financial interests or personal relationships that could have appeared to influence the work reported in this paper.

Data availability

Data will be made available on request.

Acknowledgements

We thank Sammy Bedoui (University of Melbourne) and James Vince (WEHI, Melbourne) for their help, knowledge, and guidance throughout this study and Marco Herold for his kind provision of cell lines. This work was funded by a National Health and Medical Research Council project grants to J.M.M. and P.A.W. (APP1083139 and APP1123135), and to K.E.L. (APP1162765, APP1181089). K.E.L. is an Australian Research Council (ARC) Future Fellow (FT190100266).

Appendix A. Supplementary data

Supplementary data to this article can be found online at https://doi.org/10.1016/j.virol.2023.109921.

References

Ahmed, S.M., Hall, A.J., Robinson, A.E., Verhoef, L., Premkumar, P., Parashar, U.D., Koopmans, M., Lopman, B.A., 2014. Global prevalence of norovirus in cases of gastroenteritis: a systematic review and meta-analysis. Lancet Infect. Dis. 14, 725–730.

Aktepe, T.E., Deerain, J.M., Hyde, J.L., Fritzlar, S., Pearson, J., White, P.A., Mackenzie, J. M., 2023. Norovirus NS3 protein induces apoptosis through translation repression and dysregulation of BCL-2 pro-survival proteins. bioRxiv. https://doi.org/10.1101/2023.04.23.537759.

Bedoui, S., Herold, M.J., Strasser, A., 2020. Emerging connectivity of programmed cell death pathways and its physiological implications. Nat. Rev. Mol. Cell Biol. 21, 678–695.

Bok, K., Prikhodko, V.G., Green, K.Y., Sosnovtsev, S.V., 2009. Apoptosis in murine norovirus-infected RAW264.7 cells is associated with downregulation of survivin. J. Virol. 83, 3647–3656.

Dillon, C.P., Weinlich, R., Rodriguez, D.A., Cripps, J.G., Quarato, G., Gurung, P., Verbist, K.C., Brewer, T.L., Llambi, F., Gong, Y.N., Janke, L.J., Kelliher, M.A., Kanneganti, T.D., Green, D.R., 2014. RIPK1 blocks early postnatal lethality mediated by caspase-8 and RIPK3. Cell 157, 1189–1202.

Doerflinger, M., Deng, Y., Whitney, P., Salvamoser, R., Engel, S., Kueh, A.J., Tai, L., Bachem, A., Gressier, E., Geoghegan, N.D., Wilcox, S., Rogers, K.L., Garnham, A.L., Dengler, M.A., Bader, S.M., Ebert, G., Pearson, J.S., De Nardo, D., Wang, N., Yang, C., Pereira, M., Bryant, C.E., Strugnell, R.A., Vince, J.E., Pellegrini, M., Strasser, A., Bedoui, S., Herold, M.J., 2020. Flexible usage and interconnectivity of diverse cell death pathways protect against intracellular infection. Immunity 53, 533–547 e7.

Dubois, H., Sorgeloos, F., Sarvestani, S.T., Martens, L., Saeys, Y., Mackenzie, J.M., Lamkanfi, M., van Loo, G., Goodfellow, I., Wullaert, A., 2019. Nlrp3 inflammasome activation and Gasdermin D-driven pyroptosis are immunopathogenic upon gastrointestinal norovirus infection. PLoS Pathog. 15, e1007709.

Edgington, L.E., van Raam, B.J., Verdoes, M., Wierschem, C., Salvesen, G.S., Bogyo, M., 2012. An optimized activity-based probe for the study of caspase-6 activation. Chem Biol 19, 340–352.

Fritzlar, S., Jegaskanda, S., Aktepe, T.E., Prier, J.E., Holz, L.E., White, P.A., Mackenzie, J. M., 2018. Mouse norovirus infection reduces the surface expression of major histocompatibility complex class I proteins and inhibits CD8(+) T cell recognition and activation. J. Virol. 92.

Fritzlar, S., Aktepe, T.E., Chao, Y.W., Kenney, N.D., McAllaster, M.R., Wilen, C.B., White, P.A., Mackenzie, J.M., 2019. Mouse Norovirus Infection Arrests Host Cell Translation Uncoupled from the Stress Granule-PKR-eIF2alpha Axis mBio 10.

Furman, L.M., Maaty, W.S., Petersen, L.K., Ettayebi, K., Hardy, M.E., Bothner, B., 2009. Cysteine protease activation and apoptosis in Murine norovirus infection. Virol. J. 6, 139.

Harris, K.G., Morosky, S.A., Drummond, C.G., Patel, M., Kim, C., Stolz, D.B., Bergelson, J. M., Cherry, S., Coyne, C.B., 2015. RIP3 regulates autophagy and promotes Coxsackievirus B3 infection of intestinal epithelial cells. Cell Host Microbe 18, 221–232.

Herod, M.R., Salim, O., Skilton, R.J., Prince, C.A., Ward, V.K., Lambden, P.R., Clarke, I. N., 2014. Expression of the murine norovirus (MNV) ORF1 polyprotein is sufficient to induce apoptosis in a virus-free cell model. PLoS One 9, e90679.

Karst, S.M., Wobus, C.E., Lay, M., Davidson, J., Hwt, Virgin, 2003. STAT1-dependent innate immunity to a Norwalk-like virus. Science 299, 1575–1578.

Lawlor, K.E., Khan, N., Mildenhall, A., Gerlic, M., Croker, B.A., D'Cruz, A.A., Hall, C., Kaur Spall, S., Anderton, H., Masters, S.L., Rashidi, M., Wicks, I.P., Alexander, W.S., Mitsuuchi, Y., Benetatos, C.A., Condon, S.M., Wong, W.W., Silke, J., Vaux, D.L., Vince, J.E., 2015. RIPK3 promotes cell death and NLRP3 inflammasome activation in the absence of MLKL. Nat. Commun. 6, 6282.

Lee, B.L., Stowe, I.B., Gupta, A., Kornfeld, O.S., Roose-Girma, M., Anderson, K., Warming, S., Zhang, J., Lee, W.P., Kayagaki, N., 2018. Caspase-11 auto-proteolysis is crucial for noncanonical inflammasome activation. J. Exp. Med. 215, 2279–2288.

Lee, S., Liu, H., Wilen, C.B., Sychev, Z.E., Desai, C., Hykes Jr., B.L., Orchard, R.C., McCune, B.T., Kim, K.W., Nice, T.J., Handley, S.A., Baldridge, M.T., Amarasinghe, G. K., Virgin, H.W., 2019. A secreted viral nonstructural protein determines intestinal norovirus pathogenesis. Cell Host Microbe 25, 845–857 e5.

Liao, Y., Hong, X., Wu, A., Jiang, Y., Liang, Y., Gao, J., Xue, L., Kou, X., 2021. Global prevalence of norovirus in cases of acute gastroenteritis from 1997 to 2021: an updated systematic review and meta-analysis. Microb. Pathog. 161, 105259.

McFadden, N., Bailey, D., Carrara, G., Benson, A., Chaudhry, Y., Shortland, A., Heeney, J., Yarovinsky, F., Simmonds, P., Macdonald, A., Goodfellow, I., 2011. Norovirus regulation of the innate immune response and apoptosis occurs via the product of the alternative open reading frame 4. PLoS Pathog. 7, e1002413.

Orning, P., Weng, D., Starheim, K., Ratner, D., Best, Z., Lee, B., Brooks, A., Xia, S., Wu, H., Kelliher, M.A., Berger, S.B., Gough, P.J., Bertin, J., Proulx, M.M., Goguen, J. D., Kayagaki, N., Fitzgerald, K.A., Lien, E., 2018. Pathogen blockade of TAK1 triggers caspase-8-dependent cleavage of gasdermin D and cell death. Science 362, 1064–1069.

Owusu, I.A., Quaye, O., Passalacqua, K.D., Wobus, C.E., 2021. Egress of non-enveloped enteric RNA viruses. J. Gen. Virol. 102.

Pearson, J.S., Giogha, C., Muhlen, S., Nachbur, U., Pham, C.L., Zhang, Y., Hildebrand, J. M., Oates, C.V., Lung, T.W., Ingle, D., Dagley, L.F., Bankovacki, A., Petrie, E.J., Schroeder, G.N., Crepin, V.F., Frankel, G., Masters, S.L., Vince, J., Murphy, J.M., Sunde, M., Webb, A.I., Silke, J., Hartland, E.L., 2017. EspL is a bacterial cysteine protease effector that cleaves RHIM proteins to block necroptosis and inflammation. Nat Microbiol 2, 16258.

Pires, S.M., Fischer-Walker, C.L., Lanata, C.F., Devleesschauwer, B., Hall, A.J., Kirk, M. D., Duarte, A.S., Black, R.E., Angulo, F.J., 2015. Aetiology-specific estimates of the global and regional incidence and mortality of diarrhoeal diseases commonly transmitted through food. PLoS One 10, e0142927.

Polykratis, A., Hermance, N., Zelic, M., Roderick, J., Kim, C., Van, T.M., Lee, T.H., Chan, F.K.M., Pasparakis, M., Kelliher, M.A., 2014. Cutting edge: RIPK1 Kinase inactive mice are viable and protected from TNF-induced necroptosis in vivo. J. Immunol. 193, 1539–1543.

Robinson, B.A., Van Winkle, J.A., McCune, B.T., Peters, A.M., Nice, T.J., 2019. Caspase-mediated cleavage of murine norovirus NS1/2 potentiates apoptosis and is required for persistent infection of intestinal epithelial cells. PLoS Pathog. 15, e1007940.

Samir, P., Malireddi, R.K.S., Kanneganti, T.D., 2020. The PANoptosome: a deadly protein complex driving pyroptosis, apoptosis, and necroptosis (PANoptosis). Front. Cell. Infect. Microbiol. 10, 238.

Santiana, M., Ghosh, S., Ho, B.A., Rajasekaran, V., Du, W.L., Mutsafi, Y., De Jesus-Diaz, D.A., Sosnovtsev, S.V., Levenson, E.A., Parra, G.I., Takvorian, P.M., Cali, A., Bleck, C., Vlasova, A.N., Saif, L.J., Patton, J.T., Lopalco, P., Corcelli, A., Green, K.Y., Altan-Bonnet, N., 2018. Vesicle-cloaked virus clusters are optimal units for inter-organismal viral transmission. Cell Host Microbe 24, 208–220 e8.

Sarhan, J., Liu, B.C., Muendlein, H.I., Li, P., Nilson, R., Tang, A.Y., Rongvaux, A., Bunnell, S.C., Shao, F., Green, D.R., Poltorak, A., 2018. Caspase-8 induces cleavage of gasdermin D to elicit pyroptosis during Yersinia infection. Proc. Natl. Acad. Sci. U. S. A. 115, E10888-E10897.

Seo, J., Nam, Y.W., Kim, S., Oh, D.B., Song, J., 2021. Necroptosis molecular mechanisms: recent findings regarding novel necroptosis regulators. Exp. Mol. Med. 53, 1007–1017.

Shah, M.P., Hall, A.J., 2018. Norovirus illnesses in children and adolescents. Infect. Dis. Clin. 32, 103–118.

Shi, C., Cao, P., Wang, Y., Zhang, Q., Zhang, D., Wang, Y., Wang, L., Gong, Z., 2023. PANoptosis: a cell death characterized by pyroptosis, apoptosis, and necroptosis. J. Inflamm. Res. 16, 1523–1532.

Sosnovtsev, S.V., Belliot, G., Chang, K.O., Prikhodko, V.G., Thackray, L.B., Wobus, C.E., Karst, S.M., Virgin, H.W., Green, K.Y., 2006. Cleavage map and proteolytic processing of the murine norovirus nonstructural polyprotein in infected cells. J. Virol. 80, 7816–7831.

Vinje, J., Estes, M.K., Esteves, P., Green, K.Y., Katayama, K., Knowles, N.J., L'Homme, Y., Martella, V., Vennema, H., White, P.A., Ictv Report C, 2019. ICTV virus taxonomy profile: Caliciviridae. J. Gen. Virol. 100, 1469–1470.

Wang, G., Zhang, D., Orchard, R.C., Hancks, D.C., Reese, T.A., 2023. Norovirus MLKL-like protein initiates cell death to induce viral egress. Nature. https://doi.org/10.1038/s41586-023-05851-w.

Wobus, C.E., Karst, S.M., Thackray, L.B., Chang, K.O., Sosnovtsev, S.V., Belliot, G., Krug, A., Mackenzie, J.M., Green, K.Y., Virgin, H.W., 2004. Replication of Norovirus in cell culture reveals a tropism for dendritic cells and macrophages. PLoS Biol. 2, e432.